Soft Matter

Accepted Manuscript

This is an *Accepted Manuscript*, which has been through the Royal Society of Chemistry peer review process and has been accepted for publication.

Accepted Manuscripts are published online shortly after acceptance, before technical editing, formatting and proof reading. Using this free service, authors can make their results available to the community, in citable form, before we publish the edited article. We will replace this *Accepted Manuscript* with the edited and formatted *Advance Article* as soon as it is available.

You can find more information about *Accepted Manuscripts* in the **Information for Authors**.

ROYAL SOCIETY OF CHEMISTRY

www.rsc.org/softmatter

Planar Equilibrium Shapes of a Liquid Drop on a Membrane

Chung-Yuen Hui[1], Anand Jagota[2*]

[1]Cornell University, Department of Mechanical and Aerospace Engineering, Cornell University, Ithaca, NY 14850

[2]Lehigh University, Department of Chemical Engineering and Bioengineering Program, 111 Research Drive, Lehigh University, Bethlehem, PA 18015

*Corresponding Author

Abstract

The equilibrium shape of a small liquid drop on a smooth rigid surface is governed by minimization of energy with respect to change in configuration, represented by the well-known Young's equation. In contrast, the equilibrium shape near line separating three immiscible fluid phases is determined by force balance, represented by Neumann's Triangle. These two are limiting cases of the more general situation of a drop on a deformable, elastic, substrate. Specifically, we have analyzed planar equilibrium shapes of a liquid drop on a deformable membrane. We show that to determine its equilibrium shape one must simultaneously satisfy configurational energy and mechanical force balance along with a constraint on liquid volume. The first condition generalizes the Young's equation to include changes in stored elastic energy upon change in configuration. The second condition, generalizes the force balance conditions by relating tensions to membrane stretches via its constitutive elastic behavior. The transition from Young's equation to Neumann's triangle is governed by the value of the elasto-capillary number, $\beta = T_{Ro} / \mu h$, where T_{Ro} is twice the surface tension of the solid-vapor interface, μ is the shear modulus of the membrane, and h is its thickness.

1. Introduction

What is the *equilibrium* shape of a liquid drop on a smooth solid flat surface? If the solid is rigid and isotropic, gravity is negligible, and the contact line is free to sample the flat surface, then the equilibrium shape is a spherical cap with a contact angle θ_{cr} which is determined by *minimizing the free energy* of the system with respect to movement of the contact line relative to the solid surface [1, 2]. This minimization of free energy with respect to change in configuration will be referred to as *configuration energy balance* and results in the Young's equation:

$$cos\,\theta_{cr} = (\gamma_{SV} - \gamma_{SL})\,/\,\gamma_{LV}\,, \tag{1a}$$

where γ_{LV}, γ_{SV} and γ_{SL} are the surface *energies* of the liquid/vapor, solid/ vapor and solid/liquid interfaces, respectively.   The subscript in θ_{cr} denotes the rigid limit. In the other extreme, if the solid is replaced by a fluid that is immiscible with the liquid drop, then the angles at which the three fluid-fluid interfaces meet at the contact line between the three fluids (*a,b,c*) (Figure 1b) is governed by *mechanical force balance* of interfacial tensions $\sigma_{ab}, \sigma_{bc}, \sigma_{ac}$:

$$\sigma_{ab} \sin\theta_c = \sigma_{bc} \sin\theta_i \tag{1b}$$

$$\sigma_{ac} = \sigma_{ab} \cos\theta_c + \sigma_{bc} \cos\theta_i \tag{1c}$$

These equilibrium conditions (1 b,c), if represented as a set of vectors in two-dimensions, form a closed triangle (representing equilibrium) known as Neumann's Triangle[1, 2]. Because fluids by definition have no reference configuration, configurational energy balance and force balance are indistinguishable.

The situation is far from clear if the solid is deformable. That liquid surface tension can cause significant deformation in a compliant elastic solid has been known for some time [1, 3-6], and local substrate deformation due to liquid surface tension has been studied [7, 8], however, usually without accounting for the *additional* resistance to deformation offered by the interfacial surface tensions.   It turns out that for soft materials, these interfacial tensions can be a dominant force controlling the substrate deformation near the contact line [9-13]. It has been shown that as the substrate stiffness approaches rigidity, the contact angle is given by Young's equation (as required) whereas in the limit of vanishing substrate shear modulus, the angles at the contact line are given by Neumann's triangle[11-13]. In this sense, the latter is a fluid-like limit.

From the continuum perspective, it appears that two different principles are applied to determine the geometry of the contact line: configurational energy balance for an un-deformable solid and mechanical force balance when the solid has no resistance to shear.   Because the terms *configurational energy balance* and *mechanical force balance* are central to the argument developed in this paper, it is useful at the outset to clarify their meaning and the difference between the two. Figure 1(a) depicts a liquid drop on a rigid (or very stiff) substrate. The equilibrium shape of the drop must satisfy two conditions.   The first, which we call configurational energy balance, stems from the requirement that the free energy be minimized with respect to small variations of the contact line *with respect to the solid material*. This is depicted by the dashed lines in Figure 1(a) representing virtual displacements of the drop surface and the fixed red circle representing a material point in the solid body. Enforcing free energy minimization with the constraint of fixed liquid volume, which is what we mean by configurational energy balance, results in Young's equation as cited above, see also for example [14].

The second condition is that of mechanical force balance, i.e., the forces on some boundary encircling the material point (red circle) due to the liquid and from the rest of the solid must balance. This is shown by the free-body diagram of a small region surrounding the material point at the contact line in which we show the three surface tensions, $\gamma_{LV}, \sigma_{SL}, \sigma_{SV}$. The symbol γ stands for surface

energy; σ for surface tension (isotropic surface stress) – note that for a solid we distinguish between the two but they are identical for a liquid. For a rigid substrate the condition that all forces must balance is satisfied trivially or automatically because, whatever the configuration of the drop, the substrate provides the necessary reaction force to balance the forces applied by the surface tensions. (By making the region occupied by the free-body diagram very small compared to the size of the drop, we can make the contribution of the Laplace pressure negligible.) Thus, in this case, configurational energy balance alone determines the shape of the drop.

On the other hand, when the three bodies are fluids (Figure 1(b)), mechanical or force equilibrium of a small surface around the material point (red circle) determines the angles and hence the shape. However, force balance in this limit also implies configurational energy balance since surface energies numerically equal surface tensions. Thus, both principles are satisfied in both the limiting cases drawn in Figure 1.

In exactly the same way, in the general case of a deformable substrate, the mechanical forces must balance *and* the location and shape of the droplet must be such that the configuration minimizes energy (including interfacial and *elastic* contributions) for virtual changes of the contact line with respect to the solid. The difference in the case of a deformable substrate is that both force balance and configurational energy balance now must account for the contribution from elastic deformation, and potentially the difference between surface energies and surface tensions. For example, the stresses associated with elastic deformation must satisfy the equilibrium equations of mechanics and can contribute to force balance at the contact line. Likewise, one must account for the presence of elastic energy in the free energy of the system.

What is missing in the literature is that often only one of these principles is invoked, or the two are conflated which is generally not permissible. As a result, the complex interplay resulting from enforcing these two principles simultaneously has not been investigated. The key idea of this paper is to illustrate this interplay using a simple system – a liquid droplet on a thin elastic film. In a thin film geometry, the elasticity is sufficiently simple that we can allow for arbitrarily large deformation, a feature that is missing from current theoretical analyses of contact line mechanics. Also, as demonstrated by Nadermann et al. [15] a drop on an elastic film results in its bulging due to Laplace pressure, which is readily observable, so experiments can be designed to test our theory. In the following, we study the transition of contact line geometry from the rigid limit (Young's equation) to the liquid limit (Neumann's triangle) for this system.
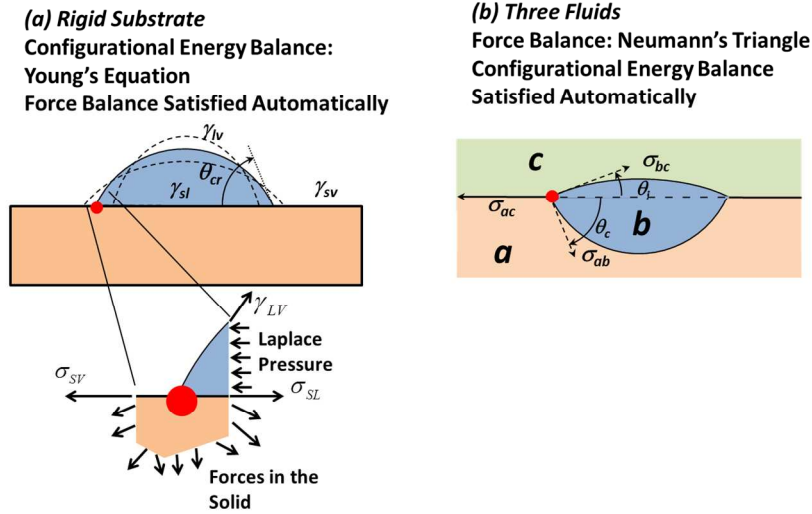
Figure 1 (a) On a rigid substrate, the equilibrium shape of a liquid drop with a free contact line is determined by configurational energy balance, by which we mean minimization of free energy for motion of the contact line with respect to the solid surface. The zoomed-in free body diagram of a region near a material point on the solid surface shows forces, whose balance is satisfied automatically because the rigid substrate provides whatever force is necessary. (b) The shape near the contact line separating three fluids is determined by balance of surface tension forces, which is consistent with configurational energy balance.

2.1   Problem Formulation:

The geometry is illustrated in Figure 2. A liquid drop is placed under a thin elastic film of initial thickness h. The film is fixed at two rigid supports a distance $2a$ apart and is so thin that bending effects can be neglected and hence it can support only in-plane tension. To make our idea as transparent as possible, we simplify the mathematics by assuming the liquid drop and the film are infinitely long in the out-of-plane direction – it deforms in plane strain. We assume that V, the volume per unit length of the drop, is sufficiently small so the effect of gravity can be neglected. The absence of external forces implies that the film *outside* the drop remains *flat*. We assume that the surfaces are isotropic and surface tension is independent of surface stretch.

Figure 2 also shows the forces applied by the liquid drop on the film/membrane. These include two line forces from the liquid surface tension at $|x| = c$ as well as a distributed Laplace pressure for $|x| < c$. The net force applied by the drop is zero, that is, the forces due to the Laplace force are balanced by the two line forces. These forces cause the film to bulge which induces stretching, as shown in Fig. 2. As shown in [16], the deformed film above the liquid drop must be a *circular arc of radius* $R_i = c / \sin \theta_i$. We denote θ_i, θ_c to be the angles made by the bulged film and the drop to the flat outer film, respectively (see Figure 2).
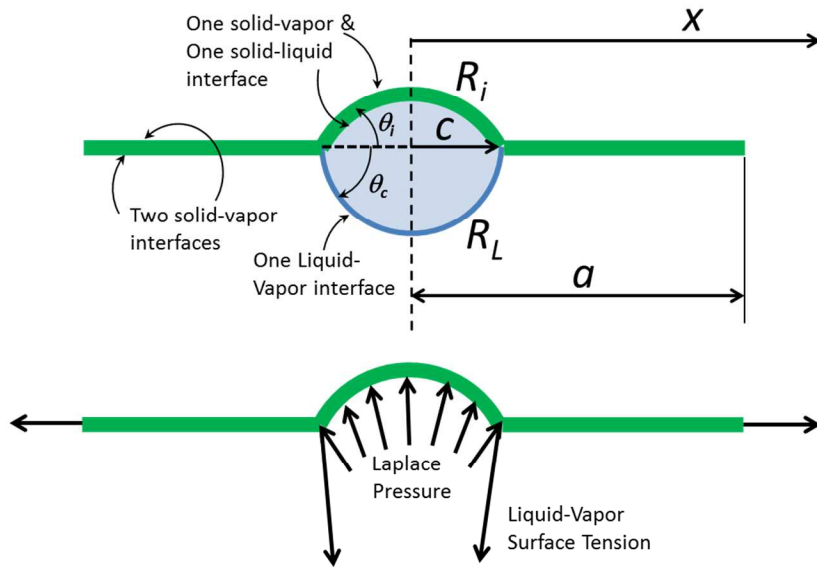
Figure 2 Schematic drawing of the system analyzed. It comprises a plane strain solid thin film (Green) spanning a gap of *2a* (and infinite in extent out of the plane). The liqud drop (shaded blue) is placed *under* the solid film. The lower part of the figure shows a free-body diagram of the solid film. The drop applies a Laplace pressure and line surface tension force, which together bulge the solid film into a circular arc of radius R_i. The film of width 2a is fixed at its edges (at $x = \pm a$). We neglect gravity in our model and, as a result, the film is flat outside the drop. The contact line occupies the lines $x = \pm c$.

The stretch of the film is measured from its reference configuration which we take to be an undeformed flat film. Let $\pm c$ and $\pm \rho_c$ denote the coordinate of the contact line in the deformed and reference configuration, respectively. Note that, after deformation, the surface of the drop is still a circular arc with radius $R_L = c / \sin \theta_i$ (see Fig. 2). The stretch ratios λ_i and λ_o measure the deformation of the film and are defined as the ratio of the deformed to undeformed length (e.g. a stretch ratio of 1 implies no deformation). These quantities take different values in the bulged (λ_i) and the flat outer (λ_o) portion of the film but are constant in each region. For example, the straight line segment $[0, \rho_c]$ deforms into the circular arc (bulge) with radius R_i and arc length $R_i \theta_i$, so the stretch ratio of the bulge is

$$\lambda_i = \frac{R_i \theta_i}{\rho_c} = \frac{c \theta_i}{\rho_c \sin \theta_i}, \qquad (2a)$$

Likewise, the stretch ratio in the flat outer portion of the film is

$$\lambda_o = \frac{a - c}{a - \rho_c} \qquad (2b)$$

To relate these elastic stretches to the tensions induced by them, the film is assumed to stretch as an ideal neo-Hookean sheet with shear modulus μ. The Neo-Hookean model is the simplest generalization of small-strain elasticity that can handle arbitrarily large deformation[17]. The

5

formulation is readily extended to other models for material elasticity.) The free energy density *W* of the film in the reference configuration has three parts. The first corresponds to interfacial surface energy, the second the work done by the surface tensions, and the last term is the elastic strain energy density. The expressions for free energy density are different for the parts inside and outside the liquid drop. They are

$$W(\lambda_i) = (\gamma_{SV} + \gamma_{SL}) + T_{Ri}(\lambda_i - 1) + \frac{\mu h}{2}\left(\lambda_i^2 + \frac{1}{\lambda_i^2} - 2\right),$$

$$W(\lambda_0) = 2\gamma_{SV} + T_{R0}(\lambda_0 - 1) + \frac{\mu h}{2}\left(\lambda_0^2 + \frac{1}{\lambda_0^2} - 2\right)$$

(3a,b)

where

$$T_{Ri} = \sigma_{SV} + \sigma_{SL}; \quad T_{Ro} = 2\sigma_{SV},$$

(3c,d)

in which terms such as γ_{SV} refer to the surface energy (solid-vapor in this case) and σ_{SV} refers to the corresponding surface tension. (The two are numerically identical for a liquid surface.) The first term in equation (3a) is the free energy density (per unit area) for creation of the two surfaces inside the region where the drop lies. The second term is the work done (per unit area) by the surface tension T_{Ri} to stretch the inner region (tension moves a distance $(\lambda_i - 1)$ per unit area). The third term is the elastic strain energy density for a Neo-Hookean solid, given its stretch[17].

The tensions T_i, T_o in and outside of the bulge are obtained by taking derivative of the corresponding expression for free energy density *W* with respect to the corresponding stretch ratios, resulting in

$$T_i = T_{Ri} + \mu h(\lambda_i - \lambda_i^{-3}); \quad T_o = T_{Ro} + \mu h(\lambda_0 - \lambda_0^{-3})$$

(4a,b)

It is important to note that the tensions and free energy densities depend on *both* surface tensions and elastic deformation.

2.2 Governing Equations: Force and Configuration energy balance

The goal is to determine the shape of the film and droplet given the surface tensions, surface energies, elastic modulus μ, a and h. Since the deflection of the film is an even function of position, we need to consider only the half of the system that occupies x > 0. As discussed previously, the contact shape is governed by two independent conditions, *force balance* and *configurational energy balance*. Horizontal and vertical force balance at the contact line require that

$$\gamma_{LV}\cos\theta_c + T_i\cos\theta_i = T_o$$

(5)

$$\gamma_{LV}\sin\theta_c = T_i\sin\theta_i$$

(6)

where T_i, T_o are given by (4a,b). Thus, the force balance has the same form as (1b,c) except the tensions are a sum of contribution from (constant) surface tensions and elastic stretches.

The second condition that must be satisfied is configurational energy balance, that is, the minimization of total free energy of the system, Γ, with respect to motion of the contact line relative to the solid film. Γ consists of the surface energy of the droplet and the free energy of the film:

$$\Gamma = \gamma_{LV}R_L\theta_c + W(\lambda_i)\rho_c + W(\lambda_0)(a - \rho_c).$$

(7)

In equation (7), the first term is the contribution of the surface energy of the liquid vapor interface. The second term is the contribution from the part of the solid film inside the drop; the third term is the contribution of the part of the solid film outside the drop. The minimization is carried out under the

constraint of fixed drop, V_0.   The shape of the drop and the deformed shape of the solid film inside the drop are both circular segments (with different radii). It is therefore simple to relate volume V_0 to the contact line half width, c.   In the reference configuration, the contact line width is c_r, the contact angle is θ_{cr} (given by Young's equation in terms of surface energies) and the volume is given by

$$V_0 = c_r^2 \ \phi(\theta_{cr}) \quad \text{where} \quad \phi(\theta) = \frac{1}{2\sin^2\theta}(\theta - \sin\theta\cos\theta) \tag{8}$$

In the deformed state, the bulge and the drop together form a circular lens of two circular segments (Fig. 2), so

$$V_0 = c^2\left[\phi(\theta_c) + \phi(\theta_i)\right]. \tag{9}$$

Differentiating the total free energy (7) with respect to c gives the configuration energy balance equation, i.e.,

$$\left.\frac{\partial\Gamma}{\partial c}\right|_{V=V_0} = 0 \tag{10}$$

Equations (5), (6), (9), and (10) are the fundamental equations governing the shape of the deformed film and the drop. The condition of configuration energy balance, (10), can also be imposed directly. A detailed analysis (Supporting Information) shows that this condition can be expressed in *closed form*:

$$T_i\left[\cos\theta_i - \lambda_i/\lambda_0\right] + \frac{W(\lambda_i) - W(\lambda_0)}{\lambda_0} + \gamma_{LV}\cos\theta_c = 0 \tag{11}$$

Equation (11) represents *configurational energy balance* and is the generalization of Young's equation (1) to the case where elastic energy changes and surface tension work associated with movement of the contact line must be considered. The three terms each represent different contributions to the change in free energy for a small virtual displacement of the contact line with respect to the solid surface; the condition of equilibrium requires that they add to zero. The first term is the change due to work of surface tension, the second terms arises because the free energy density in the solid is different inside versus outside the drop, and the third term is due to the movement of the liquid-vapor surface tension line. In the next section we show that equation (11) indeed reduces to equation (1) in the limit of a very stiff solid.   In Supporting Information, we show that (11) can be written in terms of the stretches and two important dimensionless parameters (discussed below) as

$$\left(\lambda_o^2 - \lambda_i^2\right)\left(1 + \frac{3}{\lambda_i^2\lambda_o^2}\right) + 2\beta\varepsilon = 0 \tag{12a}$$

where β is the elasto-capillary number

$$\beta = T_{Ro}/\mu h \tag{12b}$$

and

$$\varepsilon = \frac{-\gamma_{SV} + \gamma_{SL} - \sigma_{SL}}{2\sigma_{SV}} + \frac{1}{2}, \tag{12c}$$

is a dimensionless parameter that measures the difference between surface tension and energy. In particular, $\varepsilon = 0$ if surface energy equals surface tension. Although this form of the configurational energy balance equation lacks the direct connection to the physics of the problem (which equation (11) has), equation (12a) is the most useful form of the energy balance equation for analysis.   For example,

(12a) shows that $\lambda_i = \lambda_0$ if surface tension equal surface energy ($\varepsilon = 0$), a surprising result that is difficult to deduce directly from equation (11).

Normalized equations

To reduce the number of variables, we normalize all tensions, surface energies and elastic energy densities by $T_{R0} = 2\sigma_{SV}$, and lengths by the half contact length of a drop on a rigid film c_r. Thus, the constant-volume condition, eq. (9), becomes

$$1 = \overline{c}^2 \left[\frac{\phi(\theta_c)}{\phi(\theta_{cr})} + \frac{\phi(\theta_i)}{\phi(\theta_{cr})} \right], \qquad\qquad \overline{c} = c / c_r \qquad\qquad (13)$$

The normalized force-balance equations (5,6) become

$$\overline{\gamma}_{LV} \cos\theta_c + \overline{T}_i \cos\theta_i = \overline{T}_0 \qquad\qquad (14)$$

$$\overline{\gamma}_{LV} \sin\theta_c = \overline{T}_i \sin\theta_i \qquad\qquad (15)$$

where a bar over a symbol denotes normalized quantities. The tensions in (14) and (15) are given by

$$\overline{T}_i = \overline{T}_{Ri} + \frac{1}{\beta}\left(\lambda_i - \lambda_i^{-3}\right), \qquad \overline{T}_0 = 1 + \frac{1}{\beta}\left(\lambda_0 - \lambda_0^{-3}\right), \qquad\qquad (16)$$

where

$$\lambda_i = \frac{\overline{c}\theta_i}{\overline{\rho}_c \sin\theta_i}, \quad \lambda_0 = \frac{\overline{a} - \overline{c}}{\overline{a} - \overline{\rho}_c}, \quad \overline{\rho}_c = \rho_c / c_r, \quad \overline{a} = a / c_r \qquad\qquad (17)$$

Equations (12a), (13-15) are four nonlinear equations which enable us to solve for the unknown geometrical quantities $\theta_i, \theta_c, \overline{\rho}_c, \overline{c}$. The numerical procedures used to solve these equations are described in Supporting Information.

The critical dimensionless parameter that governs the physics of the problem is the elasto-capillary number $\beta = T_{Ro} / \mu h = 2\sigma_{SV} / \mu h$ (eq. 12b). When the solid film is very stiff (very large value of μ, $\beta \to 0$), we expect the system to approach the limit where contact angles are given you Young's equation (1a). When the solid film is very compliant (very small value of μ, $\beta \to \infty$), , it approaches the limit where angles are given by equations 2a and 2b. In a typical experimental realization [15], $\mu \approx 10^6\ Pa; h \approx 10^{-5}\ m; T_{Ro} \approx 10^{-1}\ N/m$, so $\beta \approx 10^{-2}$ that, as we shall see presently, is far from either limit and for which either of the limiting equations (1, 2a/2b) would be quite inaccurate. Other parameters that govern the solution are $\overline{T}_{Ri}, \overline{\gamma}_{LV}, \varepsilon$. The first two are normalized surface tension of the solid inside the drop and the normalized liquid-vapor surface tension; both are expected to be on the order of unity in value. The third parameter, ε, is zero when surface energies equal surface tensions; it thus measures departure from this condition. One of the interesting consequences of the analysis presented in this manuscript is that some aspects of the solution depend very sensitively on ε and this offers a potential experimental route to determine the difference between surface energy and surface tension.

3   Results

Before tackling the general problem of the transition from the rigid to the fluid limit, we examine the limiting case of $\beta \to 0$. In this limit we expect our formulation to revert back to Young's equation.

3.1   Rigid Limit ($\beta \to 0$, Young's Equation)

In this limit, the solid film approaches rigidity and the forces applied on it by the liquid cause negligible deformation. As a result, the film has negligible stretch both inside and outside the region covered by the drop, i.e., λ_i and λ_0 both approach 1, and $\theta_i = 0$ (the film does not deflect). Several of our equations assume simple forms. For example, the free energy density in the solid film inside and outside the drop (3a,b) now contains no contributions from either elastic energy or work of surface tension and so the difference depends only on the difference in surface energies:

$$\frac{W(\lambda_i) - W(\lambda_0)}{\lambda_0} = W(\lambda_i) - W(\lambda_0) = (\gamma_{SV} + \gamma_{SL}) - 2\gamma_{SV} = \gamma_{SL} - \gamma_{SV} \qquad (18)$$

Thus the energy balance equation (11) becomes:

$$\gamma_{SL} - \gamma_{SV} + \gamma_{LV} \cos\theta_c = 0, \qquad (19)$$

retrieving Young's equation (1a). This solution gives meaningful values of contact angle for

$-1 \geq \left(\dfrac{\gamma_{SV} - \gamma_{SL}}{\gamma_{LV}}\right) \geq 1$. At the lower limit the liquid is completely non-wetting; at the upper limit it is super-wetting and spreads.

3.2   Surface tensions equal surface energies

For materials such as elastomers and hydrogels, a typical assumption in the literature is that surface tension equals surface energy. We first consider this special case for which we can establish a few exact results. We then proceed to show results for typical parameters. For this case, $\varepsilon = 0$ and the energy balance equation (12a) can only be satisfied by the surprising result that the stretches inside and outside the drop are equal:

$$\lambda_i = \lambda_o. \qquad (20a)$$

Substituting in the expressions for the two stretches (eqs 2(a&b)),

$$\frac{\bar{c}\,\theta_i}{\bar{\rho}_c \sin\theta_i} = \frac{\bar{a} - \bar{c}}{\bar{a} - \bar{\rho}_c} \Leftrightarrow \bar{\rho} = \frac{\bar{a}}{1 + \left(\dfrac{\bar{a}}{\bar{c}} - 1\right)\dfrac{\sin\theta_i}{\theta_i}} \qquad (20b)$$

Equations (4a,b) and (20) imply that the tensions are related by:

$$T_i = T_o + \sigma_{SL} - \sigma_{SV} \Leftrightarrow \bar{T}_i - \bar{T}_o = \bar{T}_{Ri} - 1 \qquad (21)$$

that is, the *difference* in tensions is independent of elasticity. Equation (21), together with (14, 15) implies that the angles θ_i, θ_c must be related by

$$\frac{1}{\sin\theta_i}\left[\sin\theta_c - \sin(\theta_c + \theta_i)\right] = \frac{\bar{T}_{Ri} - 1}{\bar{\gamma}_{LV}} = \frac{\sigma_{SL} - \sigma_{SV}}{\gamma_{LV}} = \frac{\gamma_{SL} - \gamma_{SV}}{\gamma_{LV}} \qquad (22)$$

Equation (22) shows that while the angles no longer depend only on surface properties (since they depend on geometry and elasticity), the factor on the left hand side is a surface material property since the right hand side depends only the surface energies. It also give an explicit relation between the real contact angle $\theta_c + \theta_i$ and the angles θ_i and θ_c. Unfortunately, the angles θ_i, θ_c and $\bar{c}$ cannot be obtained in closed form and have to be determined by solving the governing equations numerically.

In general, the angles θ_i and θ_c depend on four parameters $\bar{T}_{Ri} - 1$, $\bar{\gamma}_{LV}$, β and $\bar{a}$. (Our numerical results are consistent with (22)). Figure 3(a) shows a specific example of the transition from the stiff (Young) to the compliant (Neumann Triangle) limits in which $\bar{\gamma}_{LV} = 1$ and

$\overline{\gamma}_{SL} = \overline{\sigma}_{SL} = \overline{\gamma}_{SV} = \overline{\sigma}_{SV} = 1/2$ and $\overline{a} = 5$[1]. For these parameters, in the rigid limit, $\theta_i = 0,\ \theta_c = \pi/2$ (equation 1a). This is drawn schematically in Figure 3(a) as the drop (in blue) lying under the rigid film (in green). Similarly it can also easily be shown by equations (1 b,c) that in the flexible limit $\theta_i = \theta_c = \pi/3$. Starting at the rigid limit, as one decreases film stiffness, β increases and the film angle θ_i also increases monotonically. The apparent contact angle θ_c meanwhile decreases, in accordance with (22). The real contact angle $\theta_i + \theta_c$ starts at a value of $\pi/2$ at $\beta = 0$ and reaches its compliant limit of $2\pi/3$ for values of elasto-capillary number in the 10-100 range. Going from a compliant to a stiff film, the transition to the rigid limit is slow in that it requires a very small elasto-capillary number. Note that neither the apparent contact angle nor the actual contact angle equal $\theta_{cr} = \pi/2$ except in the rigid limit. Figure 3(b) shows the stretches, tensions, $\overline{c}$ and $\overline{\rho}_c$ as a function of the elastocapillary number β. Note that the two stretches and the two tensions are identical for this case. Contact width parameters $\overline{c}$ and $\overline{\rho}_c$ do not differ much from unity.

The principal results for the case where surface tensions equal surface energies are:
- Contact angles vary smoothly between the rigid and compliant limits with increasing elastocapillary number (decreasing film stiffness),
- Except in the rigid limit, neither the apparent nor the actual contact angle equals the contact angle given by Young's equation,
- The stretch of the film inside the contact region equals that outside it,
- Although the contact angles in general *are not material properties*, a certain combination does depend only on surface energies.

---

[1] This plane strain model is meant to represent the physics of the more realistic axisymmetric drop on a membrane. A significant difference in the latter case is that the stretch in the outer part of the membrane naturally decays as 1/r so that, for our system to have roughly the same stiffness outside the contact line, a should be ~ 1-10 times c_r. We have fixed it to be five times; the results depend only weakly on this choice.

(a)   (b)
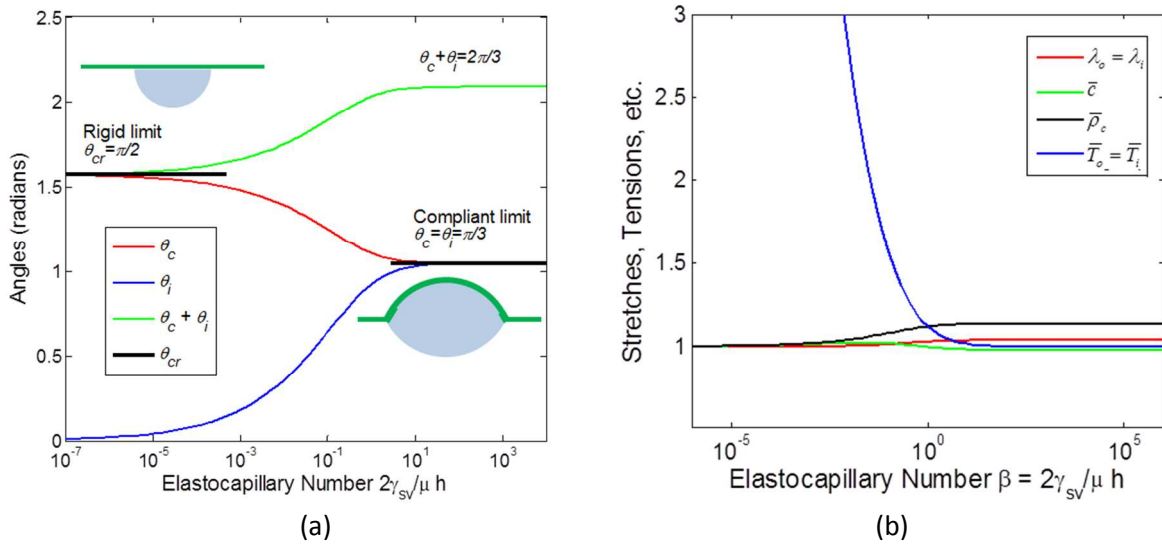
Figure 3 Results for the case when surface tensions equal surface energies. (a) Contact angles as a function of elastocapillary number. Small values of the elastocapillary number correspond to a highly stiff solid and the contact angle is given by Young's equation. Large values of the elastocapillary number correspond to a very compliant solid and the angles are given by Neumann's triangle. The transition between the two occurs over several decades of elastocapillary number. (b) Stretches, tensions, and contact width parameters as a function of elastocapillary number. Stretches and the contact width parameters do not differ much from unity, indicating modest deformation. The stretch of the solid within the contact lines is the same as that of the region outside it.

3.3   General case: Surface tension not equal to surface energy or $\varepsilon \neq 0$

A surprising and interesting result is that the stretches are very sensitive to the difference between surface energy and surface tension for compliant systems. Recall that ε measures the deviation of surface energy from surface tension, so one would expect that the solution will be close to the case of $\varepsilon = 0$ for sufficiently small ε. That this is not the case can be seen by noting that, no matter how small ε is, one can always increase β in the energy balance equation (12a) so that $\beta\varepsilon \gg 1$. Thus, as one gradually increases the film compliance (increasing β), λ_i eventually deviates from λ_0, even if the difference between surface tension and energy is very small. This divergence occurs when

$$2\beta \approx 1/|\varepsilon| \ . \tag{23}$$

The relation between λ_i and λ_0 is completely determined by the energy balance equation (12a), which can be solved to give

$$\lambda_o^2 = \frac{1}{2}\left[\left(\lambda_i^2 - \frac{1}{3\lambda_i^2} - 2\varepsilon\beta \right) + \sqrt{\left(\lambda_i^2 - \frac{1}{3\lambda_i^2} - 2\varepsilon\beta \right)^2 + 12} \right] \tag{24}$$

The positive square root sign is chosen since a negative sign will lead to complex λ_0. For sufficiently large β, (24) implies that either λ_o^2 or λ_i^2 can be very large (see Supporting Information). Thus, the inner or the outer part of the film can have very large stretches. However, since the tension due to elastic stretch is proportional to $1/\beta$ (see (16)), whereas numerically we found that the larger of the two stretches increases only as $\sqrt{2\beta\varepsilon}$, the elastic part of the tensions is expected to vanish in the flexible limit, that is, in this limit, the normalized tensions converge to

$$\bar{T}_i \to \bar{T}_{Ri}, \bar{T}_0 \to 1. \tag{25}$$

Equation (25) implies that the tensions now equal the surface tensions, i.e., in the flexible limit Neumann's triangle is recovered in its original form (eq. 1b,c).

Figures 4 and 5 plot the solutions for the case of $\varepsilon = 0.1$ and -0.1 respectively. In both cases, the angles converge to the prediction of the Young's equation for very small β and to Neumann's triangle for very large β. For large $\beta|\varepsilon|$, one of the stretches become very large $\approx \sqrt{2\beta|\varepsilon|}$ (see SI for more detail), however, the tensions remain finite because the stiffness is proportional to $1/\beta$. This is quite different than the case where surface tension = surface energy, where the stretches remain small.

(a)   (b)
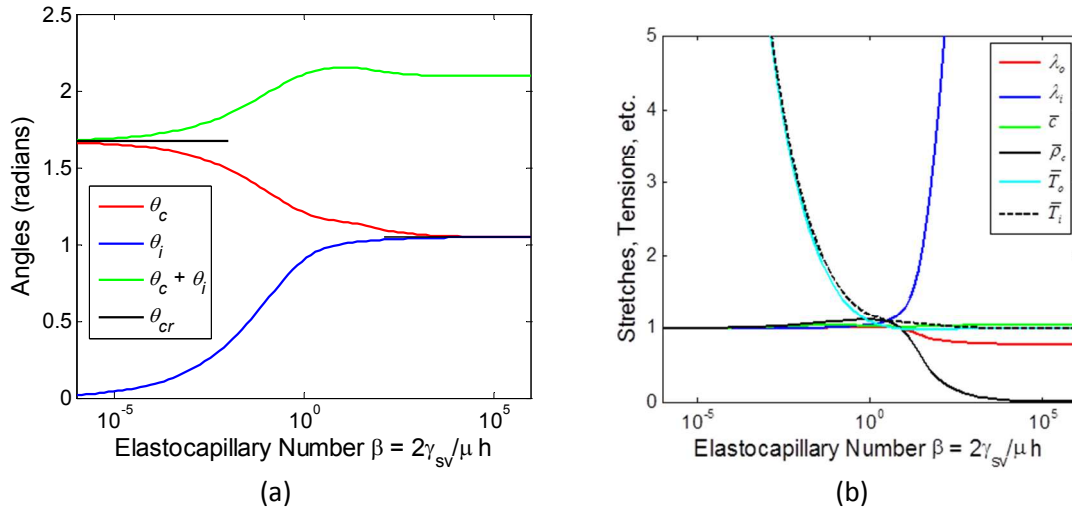
Figure 4 Results for the case where surface tensions differ in value from the corresponding surface energy. The parameters are the same as for Figure 3, except that $\bar{\gamma}_{sv} = 0.4; \ \varepsilon = 0.1$. (a) Contact angles as a function of elastocapillary number, (b) Stretches, tensions, and contact width parameters c and $\bar{\rho}_c$.

(a)   (b)
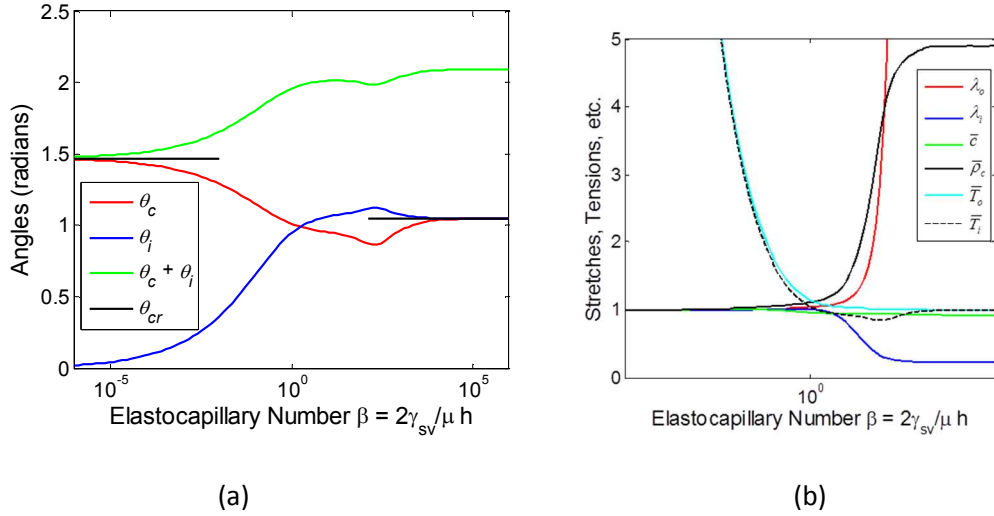
Figure 5 Results for the case where surface tensions differ in value from the corresponding surface energy. The parameters are the same as for Figure 3, except that (a) $\bar{\gamma}_{sv} = 0.6; \; \varepsilon = -0.1$. (a) Contact angles as a function of elastocapillary number, (b) Stretches, tensions, and contact width parameters c and $\bar{\rho}_c$.

Several of the results for the case where surface tensions do not equal surface energies are therefore similar to the case when surface tensions equal surface energy. The stark difference is in the extreme sensitivity of stretches to small values of a parameter that measures difference between surface tension and surface energy.

4   Summary

We have shown that the shape of wetting drops on a deformable substrate is determined by two physical conditions: force balance (in each direction), configurational energy balance representing minimization of free energy with respect to motion of the contact line relative to the solid surface, and one constraint of fixed liquid volume. In this work, we examined the special case in which the solid substrate is a thin elastic membrane. By virtue of this simplification, we are able to formulate the problem exactly. Its solution defines the shape near the liquid contact lines in terms of two angles. The formulation combines and generalizes two limiting cases. The first is the rigid limit in which the configurational energy balance condition goes to the well-known Young equation for the contact angle and force equilibrium is satisfied automatically. The second is the compliant limit in which the force balance equations go to Neumann's triangle and shape is determined by force balance alone.

Both limiting conditions are special cases of the general situation for which configurational energy balance must include contributions from elastic energy and work of moving the tension in the membrane. Similarly, the force balance equations are generalized to include contributions to the tension from elastic stretch of the membrane. Whereas in the limiting cases the contact angles depend on surface properties alone and are thus themselves material properties, in the general case of a liquid drop on a deformable substrate they are not material properties since they depend on the elasticity and geometry as well.

The more realistic case of an axisymmetric drop can be analyzed along very similar lines, although it will be mathematically more complex and less transparent. We expect, however, that the results of the plane strain problem analyzed here will differ from those of the axisymmetric drop mainly

by numerical factors without affecting the broad conclusions. The system we have modeled is also experimentally accessible, as shown by the work of Nadermann et al [15].   For example, a 1-micron thick elastomeric film with shear modulus of 100 kPa and surface tension of 50 mJ/m^2 has an elastocapillary number of one. Because the results are sensitive to the difference between surface tension and surface energy, this system could potentially be used to measure it.

5   Acknowledgement

6.   References

1.   deGennes, P.-G., F. Brochard-Wyart, and D. Quere, *Capillarity and Wetting Phenomena. Drops, Bubbles, Pearls, Waves*. 2002, New York: Springer Science+Business Media, Inc.

2.   Rowlinson, J.S. and B. Widom, *Molecular Theory Of Capillarity*. 1989, New York, USA: Oxford University Press.

3.   Carré, A., J.C. Gastel, and M.E.R. Shanahan, *Viscoelastic effects in the spreading of liquids.* 1996.

4.   Roman, B. and J. Bico, *Elasto-capillarity: deforming an elastic structure with a liquid droplet.* Journal of Physics: Condensed Matter, 2010. **22**(49).

5.   Extrand, C. and Y. Kumagai, *Contact angles and hysteresis on soft surfaces.* Journal of colloid and interface science, 1996. **184**(1): p. 191-200.

6.   Yu, Y.-S., *Substrate Elastic Deformation Due to Vertical Component of Liquid-Vapor Interfacial Tension.* Appl. Math. Mech. -Engl. Ed. , 2012. **33**(9): p. 1095-1114.

7.   Lester, G.R., *Contact angles of liquids at deformable solid surfaces.* Journal of Colloid Science, 1961. **16**(4): p. 315-326.

8.   Rusanov, A.I., *Theory of wetting of elastically deformed bodies, I. deformation with a finite contact-angle (in Russian).* Colloid Journal of the USSR, 1975. **37**(4): p. 614-622.

9.   Style, R.W., R. Boltyanskiy, Y. Che, J.S. Wettlaufer, L.A. Wilen, and E.R. Dufsresne, *Universal Deformation of Soft Substrates Near a Contact Line and the Direct Measurement of Solid Surface Stresses.* Physical Review Letters, 2013. **110**: p. 066103.

10.   Jerison, E.R., Y. Xu, L.A. Wilen, and E.R. Dufresne, *Deformation of an Elastic Substrate by a Three-Phase Contact Line.* Physical Review Letters, 2011. **106**(18): p. 186103.

11.   Marchand, A., S. Das, J.H. Snoeijer, and B. Andreotti, *Contact angles on a soft solid: from Young's law to Neumann's law.* Physical Review Letters, 2012. **109**(23): p. 236101.

12.   Hui, C.-Y. and A. Jagota, *Deformation Near a Liquid Contact LIne on an Elastic Substrate.* Proceedings of the Royal Society A: Mathematical, Physical and Engineering Science, 2014. **470**: p. 20140085.

13.   Cao, Z. and A.V. Dobrynin, *Polymeric Droplets on Soft Surfaces: From Neumann's Triangle to Young's Law.* Macromolecules, 2015. **48**(2): p. 443-451.

14.   Soligno, G., M. Dijkstra, and R. van Roij, *The equilibrium shape of fluid-fluid interfaces: Derivation and a new numerical method for Young's and Young-Laplace equations.* The Journal of Chemical Physics, 2014. **141**(24): p. 244702.

15.   Nadermann, N., C.-Y. Hui, and A. Jagota, *Solid surface tension measured by a liquid drop under a solid film.* Proceedings of the National Academy of Sciences, 2013. **110**(26): p. 10541-10545.

16.   Srivastava, A. and C.-Y. Hui, *Large deformation contact mechanics of a pressurized long rectangular membrane. II. Adhesive contact.* Proceedings of the Royal Society A: Mathematical, Physical and Engineering Science, 2013. **469**(2160).

17.   Ogden, R.W., *Non-linear elastic deformations*. 1997: Courier Corporation.